National Cheng Kung University assisted in meeting the publication costs of this article.

REFERENCES

1. M. K. Wu, J. R. Ashburn, C. J. Torng, P. H. Hor, R. L. Meng, L. Gao, Z. J. Huang, Y. Q. Wang, and C. W. Chu, *Phys. Rev. Lett.*, **58,** 908 (1987).
2. H. Maeda, Y. Tanaka, M. Fukutomi, and T. Asano, *Jpn. J. Appl. Phys.*, **27,** L209 (1988).
3. R. H. Koch, C. P. Umbach, G. J. Clark, P. Chaudhari, and R. B. Laibowitz, *Appl. Phys. Lett.*, **51,** 200 (1987).
4. G. J. Clark, A. D. Marwick, R. H. Koch, and R. B. Laibowitz, *ibid.*, **51,** 139 (1987).
5. G. J. Clark, F. K. Legoues, A. D. Marwick, R. B. Laibowitz, and R. Koch, *ibid.*, **51,** 1462 (1987).
6. B. Roas, B. Hensel, G. Saemann-Ischenko, and L. Schultz, *ibid.*, **54,** 1051 (1989).
7. K. Shiraishi, H. Itoh, and O. Yoda, *Jpn. J. Appl. Phys.*, **27,** L2339 (1988).
8. C. H. Chen, A. E. White, K. T. Short, R. C. Dynes, J. M. Poate, D. C. Jacobson, P. M. Mankiewich, W. J. Skocpol, and R. E. Howard, *Appl. Phys. Lett.*, **54,** 1178 (1989).
9. S. Matsui, H. Matsutera, T. Yoshitake, and T. Satoh, *ibid.*, **53,** 2096 (1988).
10. T. Aruga, S. Takamura, T. Hoshiya, and M. Kobiyama, *Jpn. J. Appl. Phys.*, **28,** L964 (1989).
11. O. K. Kwon, B. W. Langley, R. F. W. Pease, and M. R. Beasley, *IEEE Electron Device Lett.*, **EDL-8,** 582 (1987).
12. S. S. Lau and W. F. van der Weg, in "Thin Films-Interdiffusion and Reactions," J. M. Poate, K. N. Tu, and J. W. Mayer, Editors, p. 433, The Electrochemical Society, Princeton, NJ (1978).
13. S. M. Sze, in "Semiconductor Devices-Physics and Technology," p. 417, Bell Telephone Laboratories, Inc. (1985).
14. M. Maenpaa, L. S. Hung, M.-A. Nicolet, D. K. Sadana, and S. S. Lau, *Thin Solid Films,* **87,** 277 (1982).
15. T. Kanai, T. Kamo, and S. P. Matsuda, *Jpn. J. Appl. Phys.*, **28,** L551 (1989).
16. W. T. Lin, H. C. Chu, Y. L. Chu, H. S. Lin, Y. K. Fung, C. Y. Chang, P. T. Wu, and J. H. Kung, *Thin Solid Films,* In press.

Composition of Tungsten Silicide Films Deposited by Dichlorosilane Reduction of Tungsten Hexafluoride

Tohru Hara,* Takaaki Miyamoto, and Hiroyuki Hagiwara

Electrical Engineering, Hosei University, Kajinocho, Koganei, Tokyo 184, Japan

E. I. Bromley* and W. R. Harshbarger*

Genus Corporation, Mountain View, California 94943

ABSTRACT

The composition profile of tungsten silicide (WSi_x) films deposited by low-pressure chemical vapor deposition employing dichlorosilane (DCS) reduction of tungsten hexafluoride (WF_6) is studied. Diffusion is the reaction rate-limiting process at chuck temperatures above 550°C and uniform in-depth composition profiles can be obtained. Below 550°C, however, the in-depth composition profile is not uniform for the surface reaction rate-limiting process. Tungsten-rich layers with a Si composition, x, of 1.5, are initially deposited due to the reduction of WF_6 by the Si surface. This layer is amorphous or microcrystalline. Thereafter, the silicon content of the film increases with increasing thickness and a uniform composition profile is obtained as determined by the DCS/WF_6 flow rate ratio in the chemical reaction.

Chemical vapor-deposited tungsten silicide (WSi_x) films have been extensively used as polycide gate and interconnections for very large-scale integrated circuits (VLSI). However, peeling and cracking formation during oxidation are serious problems of the extensively used WSi_x films deposited by the silane (SiH_4) reduction (1).

The use of dichlorosilane (SiH_2Cl_2, DCS) as an alternative reducing agent to silane for tungsten hexafluoride (WF_6) has been reported (2-7). Film properties are also studied (4-7). This film has many advantageous characteristics and will be extensively used for the fabrication of VLSI WSi_x polycide gates.

In the application of this film to VLSI, the film composition is an important parameter affecting film properties such as resistivity, sheet resistance uniformity, peeling, and stress at the interface. The compositional change caused by the precipitation of excess Si at the interface during annealing has been studied in silane WSi_x films (8). Lower resistivity WSi_x films with low stress can be achieved by this precipitation. Nonuniform in-depth Si composition WSi_x films leads to sheet resistance deviation and peeling during the oxidation process. Correlation of Si composition with deposition temperature, WF_6 flow rate, and film resistivity in DCS WSi_x was studied by Gregory *et al.* (6). Although RBS spectra indicating Si composition profile were measured for DCS WSi_x by them, the relationship between in-depth Si composition profile and deposition temperature and reaction kinetics has not been studied.

It has recently been reported that the surface reaction is the rate-limiting process in the deposition of DCS WSi_x at lower temperatures (4-7). But properties of the films deposited using this reaction have not been studied.

This paper describes the properties and in-depth composition profile of WSi_x films deposited employing DCS reduction of WF_6.

Experimental Procedures

The deposition of CVD WSi_x films was performed on 5 in. (100) p-type Si using DCS reduction of WF_6. A cold-wall batch LPCVD reactor (Genus 8710) was used for the deposition of tungsten silicide. Temperature of the hot chucks was varied from 530° to 610°C. Real surface temperature of the wafer was about 30°C lower than of chuck temperature where the sheet resistance *vs.* annealing temperature relation for boron-implanted Si wafers was used for this calibration (9).

Pressure and WF_6 flow rate were varied over 0.2-0.7 torr and 9-21 sccm. The DCS flow rate was held at 670 sccm. The composition of the film was determined by 1.5 MeV $^4He^+$ Rutherford backscattering spectrometry yield ratio of Si to W (10, 11).

Thickness of WSi_x layers was determined from RBS W spectra and by a cross-sectional view of a scanning electron microscopy (SEM) measurement.

* Electrochemical Society Active Member.

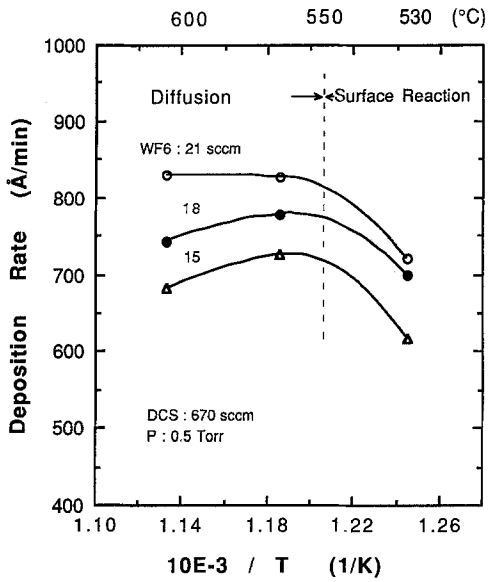

Fig. 1. Temperature variation of deposition rate for DCS WSi_x films at different WF_6 flow rate, where the DCS flow rate and pressure were held at 670 sccm and 0.5 torr, respectively.

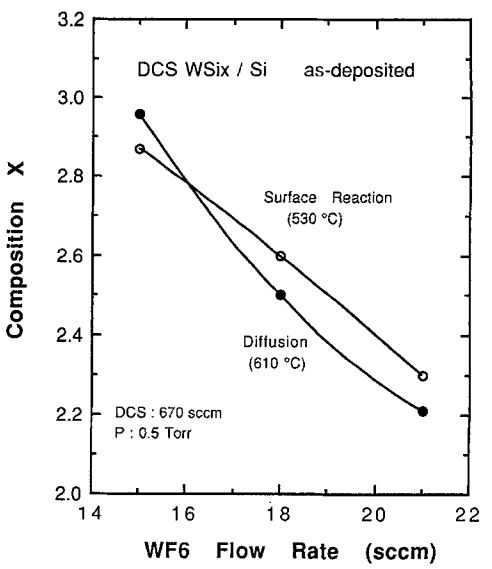

Fig. 2. Composition of DCS WSi_x films as a function of WF_6 flow rate, where the deposition was performed at chuck temperatures of 610° and 530°C, with a pressure of 0.5 torr and DCS flow rate of 670 sccm.

Results and Discussion

Deposition and film properties.—DCS WSi_x film was deposited at different chuck temperatures and WF_6 flow rates. Figure 1 shows the deposition rate as a function of the reciprocal temperature. The deposition rate for the silane film was invariable with chuck temperature over the range of 360°-425°C because diffusion is the rate-limiting process (8, 12).

In DCS WSi_x, as seen in Fig. 1, the deposition rate was independent of chuck temperature above 550°C with WF_6 flow rate of 21 sccm. This result suggests that the reactant feed rate is the deposition rate-limiting process. The deposition rate was observed to decrease with decreasing WF_6 flow rate (partial pressure). The WSi_x deposition rate is dependent on the concentration of WF_6 at the wafer surface. This decrease is mainly due to the increase of Si composition in the film due to the decrease of WF_6 gas reduced by DCS. At low WF_6 flow rates, the deposition rate decreased slowly with the increase of deposition temperature in the diffusion-limited reaction region. This decrease may be due to the increase of DCS reacted with WF_6. The rate decreased with increasing Si composition of the film.

Below a chuck temperature of 550°C, however, the deposition rate decreased exponentially with decreasing temperature, as reported previously (4-7). The reaction rate decreased when the deposition was performed at different WF_6 flow rates and pressures. These results indicate that the surface reaction is the rate-limiting process in this reaction region.

Composition of WSi_x films is an important parameter affecting film resistivity and peeling (1, 6, 8). The composition was determined by RBS analysis (10, 11). Figure 2 shows the composition at uniform regions as a function of WF_6 flow rate. Since the Si composition is limited by the amount of WF_6 reduced by DCS, the Si film composition decreases linearly with increasing WF_6 flow rate when the DCS flow rate is held constant. However, the Si composition decreased with increase in deposition temperature. This is due to the fact that the amount of DCS reacted with WF_6 increased with the increase in temperature.

Grain growth is also an important parameter in the as-deposited films (4, 6). X-ray diffraction spectra for films deposited at 610° and 530°C are shown in Fig. 3 and 4. The lower spectra in each figure are for thick WSi_x films. As seen in Fig. 3, stronger tetragonal (002) and (112) WSi_2 peaks and weaker hexagonal peaks appeared for thick films (2700Å, $x = 2.5$) deposited at 610°C by the diffusion rate-limiting reaction process.

In the surface reaction film (2500Å thick, $x = 2.6$), the intensity of the tetragonal (T) WSi_2 peak decreased and the hexagonal (H) peaks increased as seen in Fig. 4. The intensity ratio of T(112)/H(111) was 4.0 and 1.0 in diffusion and surface reaction films. Although the surface reaction films deposited at 530°C were annealed at 610°C, the spectra were invariable. These results showed that these differences in the grain size between the two layers are mainly due to the deposition process rather than to anneal temperature.

It is clear from these results that WSi_2 grains are already grown in as-deposited DCS WSi_x films, although no WSi_2 grains were observed in silane WSi_x films (13). Grain size of as-deposited DCS films deposited at different temperatures and WF_6 flow rates was determined from x-ray diffraction measurement (14). Grain size is an important parameter affecting film resistivity after anneal, as reported elsewhere (15).

Figure 5 shows the variation of grain size with composition for tetragonal (002) WSi_2 for films deposited at 610° (diffusion) and 530°C (surface reaction). As the Si-to-W ratio increased, grain size decreased gradually in the diffusion film and rapidly in the surface reaction film. This result indicates that grain size is dependent upon film composition. Larger WSi_2 grains were formed in the film

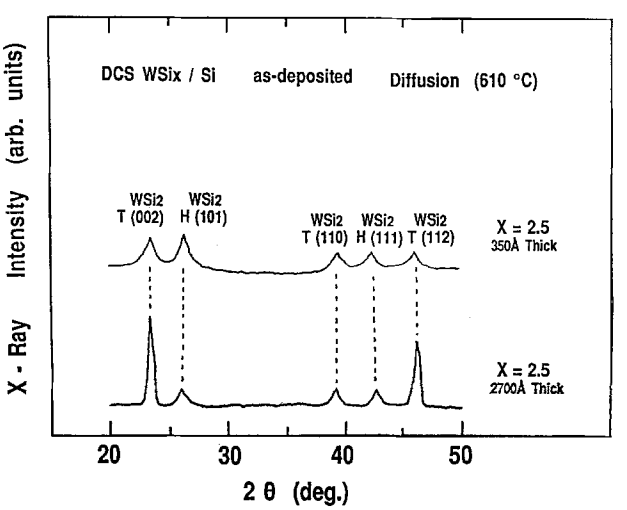

Fig. 3. X-ray diffraction spectra for thick (2700Å, in the lower trace) and thin (350Å, in the upper trace) DCS WSi_x films deposited by the diffusion rate-limiting process, where the deposition was performed at DCS and WF_6 flow rates of 670 and 18 sccm, respectively. Pressure was held at 0.5 torr.

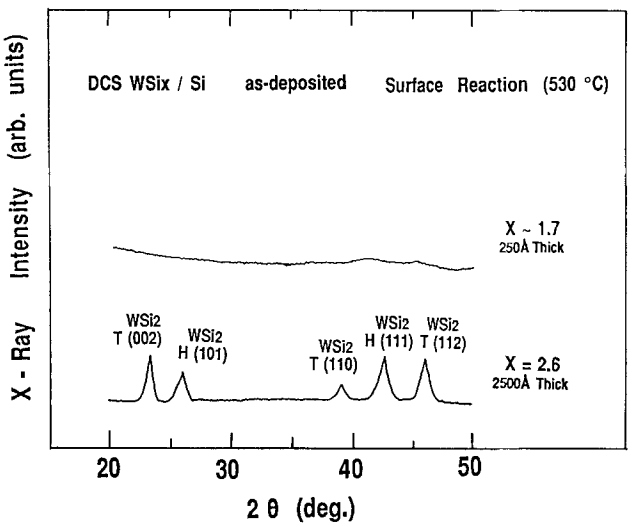

Fig. 4. X-ray diffraction spectra for thick (2500Å, in the lower trace) and thin (250Å, in the upper trace) DCS WSi_x films deposited on Si at chuck temperatures of 530°C (surface reaction), where the deposition was performed at DCS and WF_6 flow rates of 670 and 18 sccm, respectively. Pressure was held at 0.5 torr.

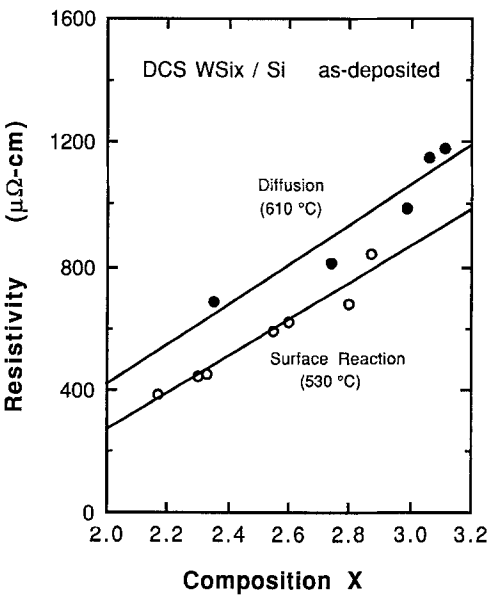

Fig. 6. Resistivity of DCS WSi_x films deposited at different chuck temperatures as a function of WF_6 flow rate, where the deposition was performed at 0.5 torr and 670 sccm.

deposited at high temperatures by diffusion rate-limiting process. The grain size of the surface reaction film was invariable after annealing at 610°C.

Sheet resistance and thickness of the film were measured by four-point probe and RBS WSi_x spectrum, respectively. Figure 6 shows the resistivity of as-deposited DCS WSi_x films as a function of film composition, where the film was deposited at a chuck temperature of 610° and 530°C. Resistivity increased with increasing Si composition. In as-deposited noncrystalline silane reduction WSi_x films, resistivity is only a function of composition (15). In DCS WSi_x films, however, WSi_2 grains are already grown in as-deposited films as shown in Fig. 3 and 4. Resistivity is function of both grain size and composition. The grain size is also a function of composition and decreases with increasing silicon composition as shown in Fig. 5.

Resistivity of as-deposited films increased with increasing silicon composition as shown in Fig. 6, although the resistivity decreased with the decrease of grain size. Lower resistivity was obtained in the surface reaction films, in spite of the fact that smaller grains were formed. This is due to the formation of a conductive, amorphous W-rich layer at the substrate interface, as is shown in Fig. 9.

Composition.—We found in the RBS film composition measurements shown in Fig. 2 that the composition profile became less uniform at the interface region as the deposition temperature was decreased. The in-depth Si composition profile for films deposited at 610° (diffusion reaction), 570°, and 530°C (surface reaction) was determined by RBS measurement and is shown in Fig. 7, where the WF_6 flow rate and pressure were 18 sccm and 0.5 torr, respectively. In this figure, the zero depth is the surface of the film. WSi_x/Si interface is also shown.

A uniform composition with thickness was obtained for films deposited by the diffusion process. In the film by the surface reaction process, however, lower Si composition layers (W-rich layers) were formed at the interface, as seen in this figure. That is, W-rich layers were formed at the initial stage of the deposition. The composition increased with subsequent deposition and uniform in-depth composition profiles were obtained in the upper film. This result shows that the reduction of WF_6 is caused by the Si surface rather than by DCS during the initial film nucleation. The reduction of WF_6 is accomplished by DCS during subsequent film deposition. In-depth composition profile measurements were performed for films deposited at different

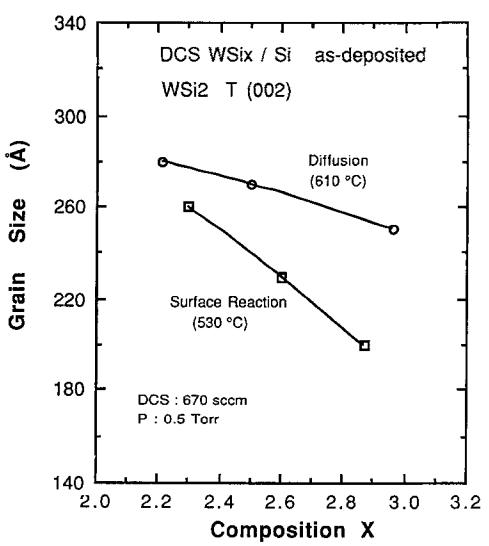

Fig. 5. Grain size of as-deposited DCS WSi_x films deposited at chuck temperatures of 610° and 530°C as a function of composition, where the deposition was performed at DCS and WF_6 flow rates of 670 and 15 to 21 sccm, respectively. Pressure was held at 0.5 torr.

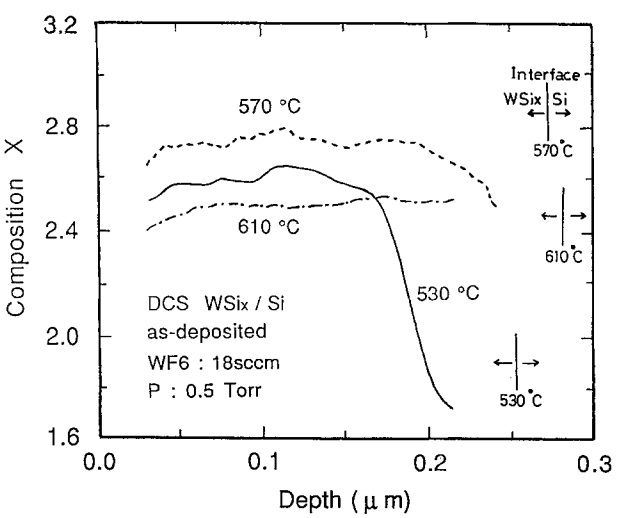

Fig. 7. In-depth composition profile of DCS WSi_x deposited on Si by surface rate-limited reaction at 530°C (surface reaction) and diffusion rate-limited reaction at 610°C. DCS and WF_6 flow rates were held at 670 and 18 sccm, respectively. Pressure was held at 0.5 torr.

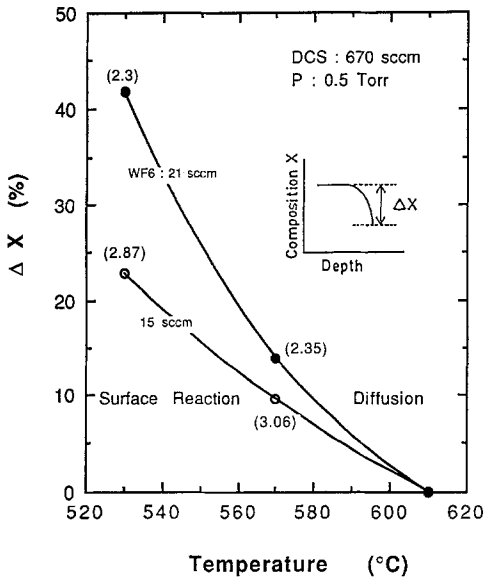

Fig. 8. Variation of the amount of composition change in the profile, Δx, with deposition temperature, where deposition was performed at 0.5 torr. Numbers in parentheses indicate the average composition of the film.

temperatures and WF_6 flow rates. The amount of composition change, Δx, defined in this figure, obtained from these measurements, is shown in Fig. 8 as function of deposition temperature, where WF_6 flow rate was 15 and 21 sccm. Numbers in parentheses are the composition at the interface. As seen in this figure, the amount of composition change, Δx, decreased with increasing deposition temperature. Tungsten-rich layers disappeared and uniform profiles were obtained when the deposition was performed at high temperature. The amount of composition change, Δx, also decreased with decrease of WF_6 flow rate. These results indicate that a uniform composition profile can be obtained when the deposition is performed at high temperatures with higher Si compositions.

Nucleated films.—Details of the film properties at the interface were studied. Thin films (around 300Å thick) were nucleated at chuck temperature of 530° and 610°C on Si with short duration deposition time (30s). Grain growth of the nucleated thin DCS WSi_x films were examined using the glancing angle x-ray diffraction technique. The spectra are shown in the upper trace of Fig. 3 and 4. Different x-ray diffraction spectra were obtained between the two thin layers. That is, small tetragonal and hexagonal WSi_2 peaks

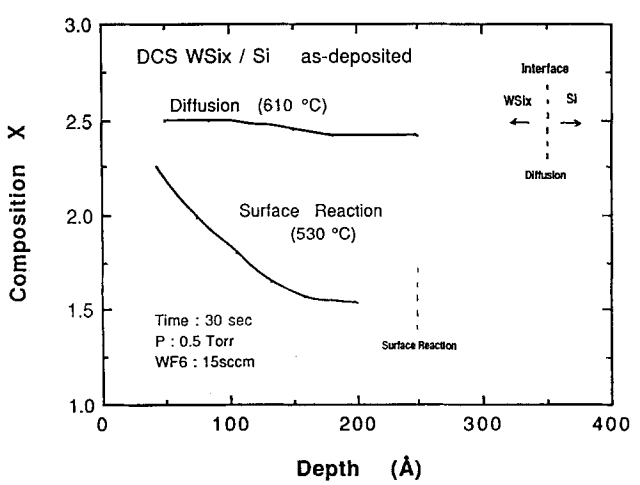

Fig. 9. In-depth composition profile for thin DCS WSi_x films nucleated on the Si surface at chuck temperatures of 530° and 610°C, where film thickness was 250 and 350Å thick for surface reaction and diffusion reaction films, respectively. The deposition was performed at DCS flow rate of 670 sccm, WF_6 flow rate 18 sccm, and pressure of 0.5 torr.

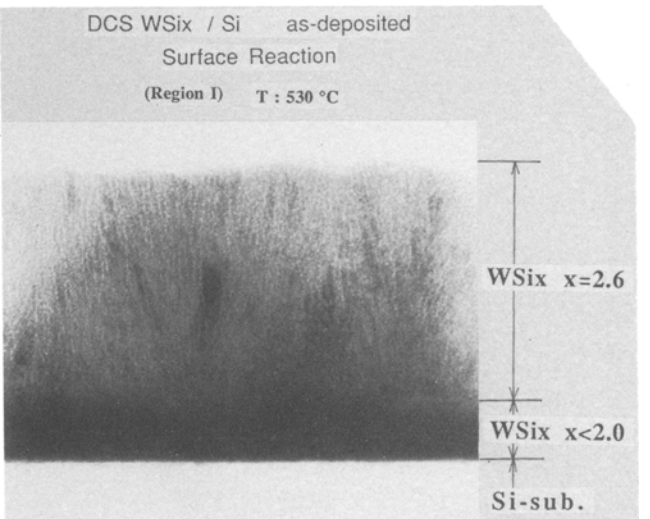

Fig. 10. Cross-sectional transmission electron micrograph of DCS WSi_x film deposited on Si at a chuck temperature of 530°C (surface reaction), where the deposition was performed at DCS flow rate of 670 sccm, WF_6 flow rate of 18 sccm, and pressure of 0.5 torr.

appeared in the thin diffusion reaction film (350Å thick) at 610°C. However, no evident peaks were observed in the thin surface reaction film (250Å thick) deposited at 530°C. Although the surface reaction film deposited at chuck temperature of 530°C was annealed at 610°C, as-deposited and annealed spectra were invariable. This result indicated that amorphous or microcrystalline layers were nucleated by surface reaction with Si.

In the diffusion reaction films shown in Fig. 3, the intensity ratio of tetragonal to hexagonal peaks, T(002)/H(101), was 1.0 in the nucleated thin film (350Å). This ratio increased to 5.0 in the thick diffusion reaction film (2700Å thick) as shown in the lower trace of Fig. 3. That is, the tetragonal WSi_2 grains were grown during the subsequent film deposition.

Exact composition profiles of the nucleated thin films formed at the interface were examined by the glancing angle RBS measurement (10). Figure 9 demonstrated the in-depth composition profile for thin films deposited by diffusion and surface reaction where film thickness was 350 and 250Å. Zero depth is the surface of the film and the interface with Si is also shown. The composition of the nucleated films was held at around 2.5 and was the same with the thick diffusion reaction film shown in Fig. 7.

However, in the thin film deposited by the surface reaction, a W-rich layer with a composition of around 1.5 was first nucleated on the Si surface. The composition increased as the thickness increased, although the DCS-to-WF_6 flow rate was held at 44.6. Such low composition films were nucleated on Si because WF_6 was reduced by the Si surface rather than by DCS. However, the reduction by the Si surface changed to DCS during subsequent film deposition. As a result, Si composition of the film increased and reached a constant with increase of thickness as seen in this figure.

The cross-sectional transmission electron microscope photograph for the film deposited from the surface reaction examined above is shown in Fig. 10. As indicated by in-depth composition profile (Fig. 9) and x-ray diffraction spectra (Fig. 4), the dark area at the interface is a W-rich amorphous layer nucleated by the surface reaction. The film changed to a crystalline layer as the film increased as seen in this photograph and in Fig. 4. WSi_2 grains can be seen in the uniform composition region.

Conclusions

The following conclusions were obtained from these experiments.

1. When deposition of DCS WSi_x film was performed at different chuck temperatures above 550°C, diffusion was the rate-limiting reaction process. Uniform, in-depth composition profiles were obtained.

2. In surface reaction rate-limiting deposition, which occurred at chuck temperatures below 550°C, a W-rich amorphous layer is formed at the interface with the Si substrate. This layer is nucleated by the surface reaction of WF_6 with Si. Nonuniform, in-depth Si composition profiles become more uniform with increase of deposition temperature.
3. The nucleated layers on Si by the surface reaction are amorphous with the Si composition, x, below 2.0. These results indicate that control of the surface reaction is needed to deposit films with a uniform composition profile.

Manuscript submitted Nov. 17, 1989; revised manuscript received April 13, 1990.

Hosei University assisted in meeting the publication costs of this article.

REFERENCES

1. K. Sakiyama, International Symposium Ion Beam Technology, Hosei University, p. 423, Hosei University Press, Tokyo, Japan (1988).
2. J. B. Price, S. Wu, Y. Chow, and J. Mendoca, *Semicon. West* (1986).
3. S. Selbrede, *Semicond. Int.*, **11**, 88 (August 1988).
4. T. Hara, T. Miyamoto, and T. Yokoyama, *Jpn. J. Appl. Phys.*, **27**, L.1812 (1988).
5. T. H. Wu, R. S. Rosler, B. C. Lartine, R. B. Gregory, and H. G. Tomskins, *J. Vac. Sci. Technol.*, **B6**, 1707 (1988).
6. R. B. Gregory, T. H. Tom Wu, H. G. Tomskins, and B. C. Lartine, *Surf. Interface Anal.*, **14**, 13 (1989).
7. T. Hara, T. Miyamoto, and T. Yokoyama, *This Journal*, **136**, 1177 (1989).
8. T. Hara, H. Takahashi, and Y. Ishizawa, *ibid.*, **134**, 1302 (1987).
9. K. Sakiyama, Private communication.
10. W-K. Chu, J. W. Mayer, and M-A. Nicolet, "Backscattering Spectrometry," p. 204, Academic Press, New York (1978).
11. T. Hara, S. Enomoto, and T. Jinbo, *Jpn. J. Appl. Phys.*, **23**, 455 (1984).
12. T. Hara, T. Miyamoto, and H. Hagiwara, Proceedings of the 1989 W Workshop of Japan, "Tungsten and Other Refractory Metals for VLSI Application."
13. K. C. Saraswat, D. L. Brors, J. A. Fair, K. A. Monnig, and R. Beyers, *IEEE Trans. Electron Devices*, **ED-30**, 1497 (1983).
14. B. D. Cullity, "Element of X-ray Diffraction," Addison-Wesley, Reading, MA (1978).
15. T. Hara, H. Hayashida, and S. Takahashi, *This Journal*, **135**, 970 (1988).

Luminescence and Energy Transfer Phenomena in Ce^{3+}, Tb^{3+} Doped $K_3La(PO_4)_2$

A. M. Srivastava,*,[1] M. T. Sobieraj, A. Valossis,** S. K. Ruan,[2] and E. Banks***

Department of Chemistry, Polytechnic University, Brooklyn, New York 11201

ABSTRACT

Energy transfer from Ce^{3+} to the Tb^{3+} ion has been observed in $K_3La(PO_4)_2$. It is shown that energy migration among the Ce^{3+} ions is of no consequence as a result of which the transfer characteristics can be described adequately by a single step Ce^{3+} to Tb^{3+} energy transfer. The critical distance of this transfer is estimated at 6.5Å. A model is used to explain the $I_{Tb^{3+}}/I_{Ce^{3+}}$ intensity ratio with increasing Tb^{3+} concentrations in $K_3La_{0.99-x}Ce_{0.01}Tb_x(PO_4)_2$.

Energy transfer from Ce^{3+} to Tb^{3+} ions in inorganic solids has been a subject of numerous investigations. This is because phosphors showing Ce^{3+}-Tb^{3+} energy transfer may be used industrially as green components in low pressure mercury vapor lamps. Further, these two rare earth elements, combined as activators in a LaOBr matrix, give an efficient green emitting phosphor, which can be used for x-ray intensifying screens (1-3).

According to Dexter's theory (4) the efficiency of energy transfer is mainly determined by the overlapping between the Ce^{3+} emission and Tb^{3+} excitation spectra.

In this communication we correlate the rare earth distribution within the cationic sublattice of the orthophosphate $K_3La(PO_4)_2$ with regard to the Ce^{3+}-Tb^{3+} energy transfer and quantitatively evaluate this transfer in this host.

The structure of $K_3La(PO_4)_2$, which is isomorphous to $K_3Nd(PO_4)_2$, has been described by Hong and Chinn (5). This compound crystallizes in the monoclinic system with space group $P2_1/m$ ($Z = 2$). The basic structural units are isolated PO_4 tetrahedra and isolated LaO_7 linkages to three pairs of La atoms at distances of 4.892, 5.652, and 6.289Å, respectively. The La site, which has mirror symmetry, is surrounded by seven oxygen atoms, of which six are near inversion positions.

Experimental

Polycrystalline samples have been prepared from stoichiometric mixtures of K_2CO_3, rare earth oxides (99.99%, Aesar Chemicals), and $NH_4H_2PO_4$ in essentially the same manner as described in Ref. (5). This consisted in preheating the mixtures at 200° for 5h to decompose K_2CO_3, and holding the temperature overnight at 1220°C to convert any metaphosphate to orthophosphate. Two heating periods, with intermittent grinding, in an atmosphere of pure and dry nitrogen, followed by final annealing at 1200°C under 97% N_2-3% H_2 atmosphere gave single-phase materials as evidenced by their x-ray diffraction patterns (CuK radiation, Philips automated diffractometer system).

Heat-treatment under reducing atmosphere is essential in order to avoid the presence of tetravalent cerium or terbium in the materials. It has been demonstrated that the Ce^{4+} and Tb^{4+} ions, in spite of their weak concentration, could play the role of energy trapping defects in some orthophosphate hosts (6).

Optical measurements were carried out as described in Ref. (7).

Results and Discussion

Ce^{3+} luminescence in $K_3La_{0.95}Ce_{0.05}(PO_4)_2$ for $0 < x < 0.20$.— The Ce^{3+} ions shows efficient ultraviolet luminescence in this host lattice. As an example Fig. 1 shows the Ce^{3+} emission (λ_{exc} = 310 nm) and excitation (λ_{em} = 337 nm) spectra of $K_3La_{0.95}Ce_{0.05}(PO_4)_2$.

At room temperature, the excitation spectrum consists of a broad band centered at 310 nm. Excitation into this band yields the emission spectrum which is clearly a doublet. The energy difference between the two emission maxima is roughly 2000 cm^{-1} and corresponds to the energy difference between the spin-orbit split $^2F_{5/2}$ and $^2F_{7/2}$ ground states.

We evaluated the dependence of Ce^{3+} emission intensity against the Ce^{3+} concentration in $K_3La_{1-x}Ce_x(PO_4)_2$ only in

* Electrochemical Society Active Member.
** Electrochemical Society Student Member.
[1] Present address: General Electric Research Laboratory, Schenectady, New York 12301.
[2] Present address: Department of Chemistry, Beijing University, Beijing, China.